

REPORT DOCUMENTATION PAGE			Form Approved OMB NO. 0704-0188		
<p>The public reporting burden for this collection of information is estimated to average 1 hour per response, including the time for reviewing instructions, searching existing data sources, gathering and maintaining the data needed, and completing and reviewing the collection of information. Send comments regarding this burden estimate or any other aspect of this collection of information, including suggestions for reducing this burden, to Washington Headquarters Services, Directorate for Information Operations and Reports, 1215 Jefferson Davis Highway, Suite 1204, Arlington VA, 22202-4302. Respondents should be aware that notwithstanding any other provision of law, no person shall be subject to any penalty for failing to comply with a collection of information if it does not display a currently valid OMB control number. PLEASE DO NOT RETURN YOUR FORM TO THE ABOVE ADDRESS.</p>					
1. REPORT DATE (DD-MM-YYYY) 13-01-2015		2. REPORT TYPE Final Report		3. DATES COVERED (From - To) 1-Oct-2013 - 30-Sep-2014	
4. TITLE AND SUBTITLE Final Report: A New Quantitative 3D Imaging Method for Characterizing Spray in the Near-field of Nozzle Exits			5a. CONTRACT NUMBER W911NF-13-2-0048		
			5b. GRANT NUMBER		
			5c. PROGRAM ELEMENT NUMBER 611102		
6. AUTHORS Rebecca Fahrig, John Eaton, Michael Benson, Pablo Vasquez Guzman			5d. PROJECT NUMBER		
			5e. TASK NUMBER		
			5f. WORK UNIT NUMBER		
7. PERFORMING ORGANIZATION NAMES AND ADDRESSES Stanford University 3160 Porter Drive, Suite 100  Palo Alto, CA 94304 -8445			8. PERFORMING ORGANIZATION REPORT NUMBER		
9. SPONSORING/MONITORING AGENCY NAME(S) AND ADDRESS (ES) U.S. Army Research Office P.O. Box 12211 Research Triangle Park, NC 27709-2211			10. SPONSOR/MONITOR'S ACRONYM(S) ARO		
			11. SPONSOR/MONITOR'S REPORT NUMBER(S) 64070-EG.3		
12. DISTRIBUTION AVAILABILITY STATEMENT Approved for Public Release; Distribution Unlimited					
13. SUPPLEMENTARY NOTES The views, opinions and/or findings contained in this report are those of the author(s) and should not be construed as an official Department of the Army position, policy or decision, unless so designated by other documentation.					
14. ABSTRACT To assist in the development of more accurate models and understanding of liquid atomization, we have developed a new quantitative measurement technique to examine the dense near-field region of sprays using X-ray computed tomography (CT). An optimized "spray CT system" was designed using a modern conventional flat-panel tabletop conebeam X-ray CT with recommendations for further improvements in spatial resolution. Three-dimensional time-averaged liquid mass distributions have been obtained for scaled pressure swirl atomizers, which match the dimensionless parameters for typical spray applications. The results reveal three dimensional					
15. SUBJECT TERMS X-ray CT, Spray, Hollow Cone Spray, Near Field					
16. SECURITY CLASSIFICATION OF:		17. LIMITATION OF ABSTRACT	15. NUMBER OF PAGES	19a. NAME OF RESPONSIBLE PERSON	
a. REPORT	b. ABSTRACT			c. THIS PAGE	Rebecca Fahrig
UU	UU	UU		19b. TELEPHONE NUMBER	
				650-724-3559	



## Report Title

Final Report: A New Quantitative 3D Imaging Method for Characterizing Spray in the Near-field of Nozzle Exits

### ABSTRACT

To assist in the development of more accurate models and understanding of liquid atomization, we have developed a new quantitative measurement technique to examine the dense near-field region of sprays using X-ray computed tomography (CT). An optimized “spray CT system” was designed using a modern conventional flat-panel tabletop conebeam X-ray CT with recommendations for further improvements in spatial resolution. Three-dimensional time-averaged liquid mass distributions have been obtained for scaled pressure swirl atomizers, which match the dimensionless parameters for typical spray application. The results reveal three-dimensional characteristics of nominally axisymmetric sprays and provide quantitative evaluation data for high-fidelity simulations. Furthermore, preliminary comparisons have been made to standard optical measurements techniques such as Shadowgraphy and PLIF as validation.

---

**Enter List of papers submitted or published that acknowledge ARO support from the start of the project to the date of this printing. List the papers, including journal references, in the following categories:**

**(a) Papers published in peer-reviewed journals (N/A for none)**

<u>Received</u>	<u>Paper</u>
-----------------	--------------

**TOTAL:**

**Number of Papers published in peer-reviewed journals:**

---

**(b) Papers published in non-peer-reviewed journals (N/A for none)**

<u>Received</u>	<u>Paper</u>
-----------------	--------------

**TOTAL:**

**Number of Papers published in non peer-reviewed journals:**

---

**(c) Presentations**

Sowell, T., Lee, Z., Benson, M., Poppel, B., Nelson, T., Vasquez Guzman, P., Fahrig, R., Eaton, J., Hinshaw, W., Kurman, M., Tess, M., and Kweon, C. 2014, “Validation of X-Ray CT-measured Liquid Concentration against LIF,” 67th Annual Meeting of the APS Division of Fluid Dynamics, Vol. 59, Number 20.

Number of Presentations: 1.00

---

**Non Peer-Reviewed Conference Proceeding publications (other than abstracts):**

<u>Received</u>	<u>Paper</u>
01/13/2015	1.00 Pablo Vasquez Guzman, John Eaton, Rebecca Fahrig, Fillipo Coletti, Michael Benson. Near-Field Spray Measurements Using X-ray Computed Tomography, Liquid Atomization and Spray Systems (ILASS) . 17-MAY-14, . . . ,
01/13/2015	2.00 Zachary Lee, Daniel Eichner, Jonathan Tennis, Matthew Ryan, Tyler Sowell, Michael Benson, Bret Van Poppel, Thomas Nelson, Pablo Vasquez Guzman, Rebecca Fahrig, John Eaton, Waldo Hinshaw, Matthew Kurman, Chol-Bum Kweon. A Comparison of Shadowgraphy and X-ray Computed Tomography in Liquid Spray Analysis, International Mechanical Engineering Congress and Exposition. 14-NOV-14, . . . ,
<b>TOTAL:</b>	<b>2</b>

Number of Non Peer-Reviewed Conference Proceeding publications (other than abstracts):

---

**Peer-Reviewed Conference Proceeding publications (other than abstracts):**

<u>Received</u>	<u>Paper</u>
-----------------	--------------

**TOTAL:**

Number of Peer-Reviewed Conference Proceeding publications (other than abstracts):

---

**(d) Manuscripts**

<u>Received</u>	<u>Paper</u>
-----------------	--------------

**TOTAL:**

**Number of Manuscripts:**

---

**Books**

Received      Book

**TOTAL:**

Received      Book Chapter

**TOTAL:**

**Patents Submitted**

---

**Patents Awarded**

---

**Awards**

---

**Graduate Students**

<u>NAME</u>	<u>PERCENT SUPPORTED</u>	<u>Discipline</u>
Pablo Vasquez Guzman	0.50	
<b>FTE Equivalent:</b>	<b>0.50</b>	
<b>Total Number:</b>	<b>1</b>	

**Names of Post Doctorates**

<u>NAME</u>	<u>PERCENT SUPPORTED</u>
<b>FTE Equivalent:</b>	
<b>Total Number:</b>	

### Names of Faculty Supported

<u>NAME</u>	<u>PERCENT SUPPORTED</u>	National Academy Member
John K. Eaton	0.00	
Rebecca Fahrig	0.00	
Michael Benson	0.00	
<b>FTE Equivalent:</b>	<b>0.00</b>	
<b>Total Number:</b>	<b>3</b>	

### Names of Under Graduate students supported

<u>NAME</u>	<u>PERCENT SUPPORTED</u>	Discipline
Zachary Lee	0.00	Mechanical Engineering
John Beck	0.00	Mechanical Engineering
Tyler Sowell	0.00	Mechanical Engineering
Zachary Glass	0.00	Mechanical Engineering
<b>FTE Equivalent:</b>	<b>0.00</b>	
<b>Total Number:</b>	<b>4</b>	

### Student Metrics

This section only applies to graduating undergraduates supported by this agreement in this reporting period

The number of undergraduates funded by this agreement who graduated during this period: ..... 0.00

The number of undergraduates funded by this agreement who graduated during this period with a degree in science, mathematics, engineering, or technology fields:..... 0.00

The number of undergraduates funded by your agreement who graduated during this period and will continue to pursue a graduate or Ph.D. degree in science, mathematics, engineering, or technology fields:..... 0.00

Number of graduating undergraduates who achieved a 3.5 GPA to 4.0 (4.0 max scale):..... 0.00

Number of graduating undergraduates funded by a DoD funded Center of Excellence grant for Education, Research and Engineering:..... 0.00

The number of undergraduates funded by your agreement who graduated during this period and intend to work for the Department of Defense ..... 4.00

The number of undergraduates funded by your agreement who graduated during this period and will receive scholarships or fellowships for further studies in science, mathematics, engineering or technology fields:..... 0.00

### Names of Personnel receiving masters degrees

<u>NAME</u>	
Pablo Vasquez Guzman	
<b>Total Number:</b>	<b>1</b>

### Names of personnel receiving PHDs

<u>NAME</u>	
<b>Total Number:</b>	

### Names of other research staff

<u>NAME</u>	<u>PERCENT SUPPORTED</u>
Waldo Hinshaw	0.15
<b>FTE Equivalent:</b>	<b>0.15</b>
<b>Total Number:</b>	<b>1</b>

---

**Sub Contractors (DD882)**

**Inventions (DD882)**

**Scientific Progress**

See Attachment.

**Technology Transfer**

This was a collaborative project between Stanford, USMA, and the Army Research Lab. There has been regular interchange including visits to Stanford and ARL by participants. The data sets have been transferred to Convergent Science, a CFD software company and we have been interacting with them through Dr. Luis Bravo of ARL.

## **A New Quantitative 3D Imaging Method for Characterizing Spray in the Near-field of Nozzle Exits**

Dr. Rebecca Fahrig, P.I.  
Department of Radiology, Stanford University  
fahrig@stanford.edu

Dr. John Eaton, Co-Investigator  
Department of Mechanical Engineering, Stanford University  
eatonj@stanford.edu

Dr. Michael Benson, Co-Investigator  
Department of Civil and Mechanical Engineering, West Point  
Michael.Benson@usma.edu

Pablo A. Vasquez Guzman  
Department of Mechanical Engineering, Stanford University  
pabloavg@stanford.edu

The development and validation of a new quantitative three-dimensional imaging technique for the dense near-field of liquid sprays based on X-ray computed tomography was proposed and has been funded since October 1<sup>st</sup>, 2013. The specific aims of Year 1 of this project were:

1. To refine and optimize our measurement system, to provide maximum image quality, including:
  - Investigate fundamental system limits of resolution, noise and reproducibility, while optimizing parameters (within the available range) for the current CT imaging system
  - Redesign and refine the air co-flow in the CT compatible flow rig to further reduce liquid accumulation on internal surfaces and validate assumptions of ‘no effect’ of co-flow system on spray distribution
2. To measure and validate mass distribution of spray (iodinated contrast) generated by a scaled nozzle, including:
  - Design a scaled up nozzle which matches the dimensionless parameters for a typical spray application.
  - Test a range of available fluids for X-ray attenuation and identify relevant criteria for selection based on cost, physical properties, and signal-to-noise ratio (SNR). In addition, fluids will also be compared based on measured physical properties to match the correct range of key non-dimensional parameters for the scaled up nozzle to include potential development of novel solutions which maximize desirable quantities for this application
  - Compare far-field mass density of the liquid phase, location of onset of atomization, and spray cone angle against currently available imaging techniques such as Shadowgraph and Mie scattering for this nozzle and fluid

The overall goal of the project was to develop and demonstrate a system with the best spatial resolution and the lowest measurement uncertainty for quantitative measurements of the liquid mass distribution. At the end of Year 1 of the project, we have generated an optimized design for a ‘spray CT system’ with recommendations for further improvements in spatial resolution. In addition to the proposed work, we have initiated collaborations with multiple groups who are developing the capability for fully resolved spray simulations. The availability of 3D, near-field measurements has made our experiments an attractive test case for model developers focusing on the primary atomization region of the spray.

## CT Imaging System

In X-ray computed tomography (CT), a three dimensional time-averaged image of the distribution of density is generated by digitally processing a series of two-dimensional projections taken around a single axis of rotation. The basic principle of X-ray CT is illustrated in Figure 1. For medical X-ray CT systems, the typical energy range of the X-ray photons generated is roughly between 20 keV and 140 keV. Within this energy range, the main interaction between X-ray photons and matter is absorption. The monochromatic behavior achieved for sprays allows for reliable measurement of its liquid mass distribution.

The spatial resolution of a CT system is determined principally by the size of the X-ray focal spot and the size and number of detector elements. The image quality of a CT system depends primarily on the settings and physical constraints of the CT system. A low photon energy level is needed to allow for sufficient penetration and attenuation. In addition, a large photon flux is needed when imaging an object with small voxel size to obtain sufficient signal-to-noise. Maximum image quality requires the lowest kVp available with the highest photon flux possible without saturating the detector. Furthermore, several geometrical parameters affect the image quality. Maximum image quality requires placing the imaged object as close to the detector and the X-ray source and detector as far apart as possible.

The experimental measurements were performed on a flat-panel tabletop cone-beam CT system in the Radiology Department at Stanford University. The X-ray generator (CPI, Canada) has a 100 kW power supply (Indico-100) with a range 40-150 kV and 10-1000 mA in radiographic mode. The X-ray tube is a Varian G-1593bi with a B-180H housing and a 0.3 mm focal spot size. The detector is a Varian PaxScan 4030CB amorphous silicon digital detector. Figure # shows image of the experimental setup.

For the present measurements, the X-ray tube was operated at 40 kVp and 80 mA to allow significant absorption of the spray and sufficient penetration through the atomizer and spray chamber. The X-ray source-to-detector distance is approximately 1420 mm and the source-to-rotation axis distance is approximately 1190 mm. A 2-by-2 binning was applied to the detector, which produces projection images of 1024 by 768 pixels. To ensure high signal-to-noise ratio, 16 sequential CT acquisitions were taken for each pressure swirl atomizer. For a single CT acquisition, 1250 equally spaced projections around a 360° rotation were acquired at an acquisition frequency of 15 frames per second. The final averaged reconstructed voxel size was  $325 \times 325 \times 325 \mu\text{m}^3$ .

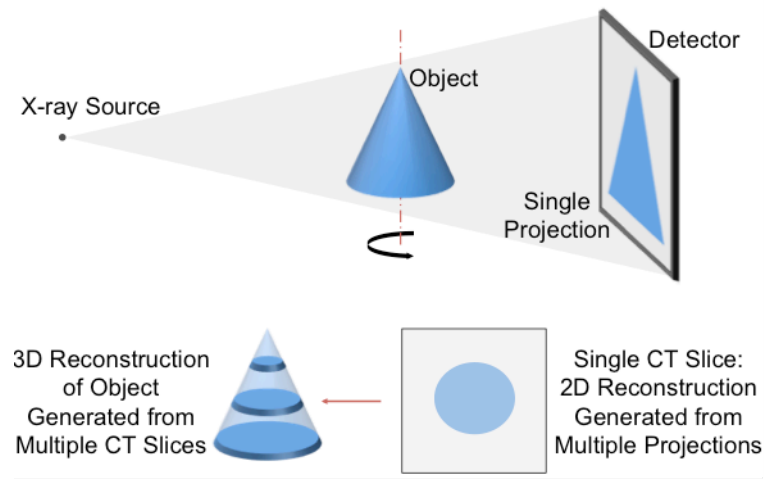


Figure 1: Basic Principle of X-ray CT system



Figure 2: Experimental Setup

## Co-Flow System

To contain the spray and avoid contamination of the laboratory the pressure swirl atomizer is contained within a cylindrical chamber. Droplet accumulation along the chamber walls is minimized using a co-flow system with air. Preliminary data were acquired using a relatively simple co-flow system design, which did not provide sufficient entrainment to prevent droplet accumulation. A redesigned co-flow flow system, which provided further reduction of liquid accumulation, was constructed. A schematic of the experimental setup is shown in Figure 3. The spray chamber is mounted on a rotating stage, which is driven by a stepper motor to allow the pressure swirl atomizer to rotate while the X-ray source and detector stayed stationary, so that multiple radiography projections could be taken from different direction of observation.

To validate the assumption that the co-flow system has “no-effect” on the spray distribution experimental measurements were acquired with and without the co-flow system. Figure 3 shows circumferentially averaged liquid concentration measured at various positions downstream of the 2 mm pressure swirl atomizer exit orifice with and without the co-flow system. The results show minimal effect on the spray characteristics with the co-flow system.

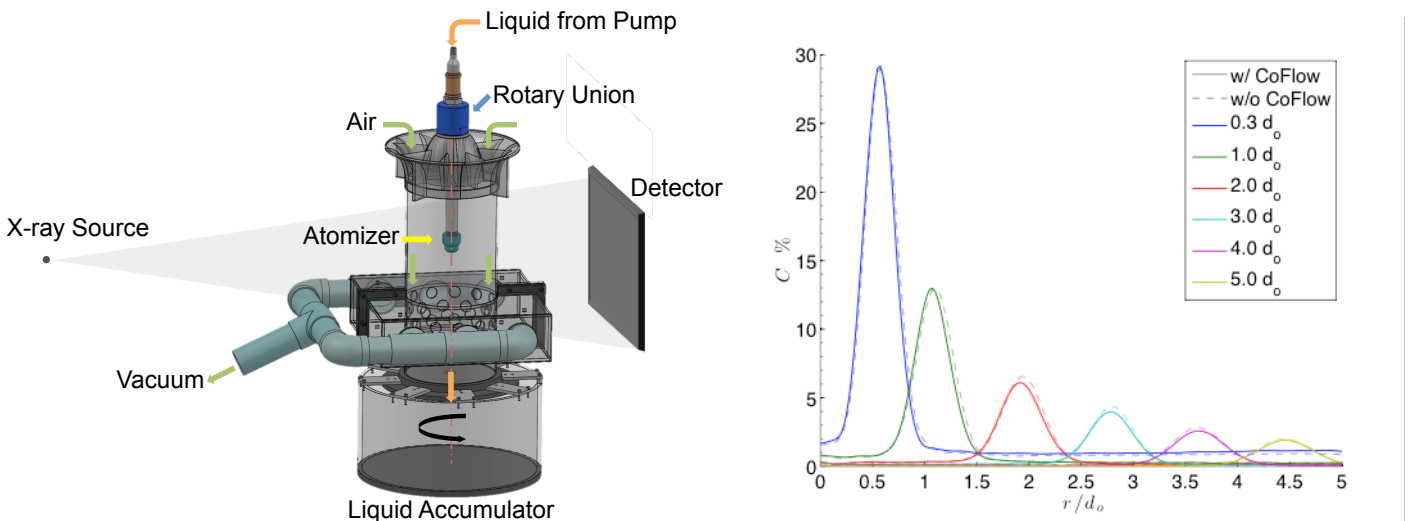


Figure 3: (a) Schematic of experimental setup (b) Circumferentially averaged liquid concentration at various nozzle diameters downstream of 2mm pressure swirl atomizer with and without co-flow system

## Pressure Swirl Atomizer

Liquid-fuel atomizers typically operate in high temperature and pressure environments, which would require the use of a heavy-duty pressure chamber to produce the environmental conditions in a laboratory setting. The presence of a thick metallic chamber is not compatible with low-energy X-ray diagnostics. In addition, the typical orifice diameter of liquid-fuel atomizers ranges around  $150\ \mu\text{m}$ , which would result in measurements with relatively low spatial resolution. To guarantee dynamic similarity with the original application of liquid fuel atomizers and high spatial resolution, a dimensionless analysis was performed to design scaled pressure swirl atomizers that operate in ambient conditions with commonly available X-ray attenuating fluids.

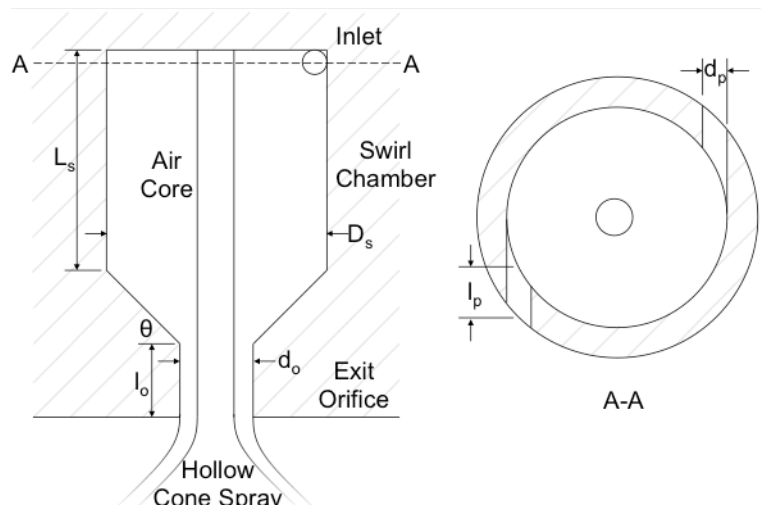


Figure 4: Typical geometry and spray features for a pressure swirl atomizer

Pressure swirl atomizers are widely used in numerous applications due to their good atomization characteristics and relative simplicity. Figure 4 shows the typical geometry and spray features of a pressure swirl atomizer. Its performance is directly influenced by its geometrical design. The effects of dimensionless geometric parameters such as  $L_s/D_s$ ,  $D_s/d_o$ ,  $l_p/d_p$ ,  $d_o/l_o$ , and  $\theta$  on atomizer performance have been studied extensively. Based on previous studies, the base line pressure atomizer is considered to have dimensionless geometric parameters of  $L_s/D_s = 1$ ,  $D_s/d_o = 3$ ,  $l_p/d_p = 1.6$ ,  $d_o/l_o = 1$ , and  $\theta = 45^\circ$ . Two pressure swirl atomizers, with orifice diameters of 2 mm and 3 mm were manufactured using stereolithography (SLA) to ensure high geometrical accuracy. Table 4 lists the dimensions of the SLA manufactured pressure swirl atomizers.

A dynamically similar pressure swirl atomizer requires the use of dimensionless parameters that characterize that atomization process. Lefebvre [1] has organized the most important dimensionless parameters, which are Reynolds number, Weber number, and discharge coefficient. By performing the dimensionless analysis, we were able to design dynamically similar pressure swirl atomizers that are at least ten times bigger than a practical pressure swirl atomizer.

Dimensional Parameter	2 mm Atomizer	3 mm Atomizer
$d_o$	2 mm	3 mm
$l_o$	2 mm	3 mm
$D_s$	6 mm	9 mm
$L_s$	6 mm	9 mm
$d_p$	1.2 mm	1.8 mm
$l_p$	2 mm	3 mm
$\theta$	45°	45°
# Inlets	2	3

Dimensionless Parameter	Definition	Typical Values	Present Values	
			2 mm Atomizer	3 mm Atomizer
$Re$	$\frac{\rho u d}{\mu}$	$6.5 \cdot 10^3$	$2.64 \cdot 10^3$	$3.96 \cdot 10^3$
$We$	$\frac{\rho u^2 d}{\sigma}$	$1.1 \cdot 10^5$	$0.11 \cdot 10^5$	$0.17 \cdot 10^5$
$C_D$	$\frac{\dot{m}}{A_o \sqrt{\Delta P \rho}}$	0.29	0.21	0.26

Table 1: (a) Pressure swirl atomizer dimensions (b) Typical values and present values of dimensionless parameters

## Liquid Analysis

Contrast agents are commonly used to improve the image quality and dynamic range of X-ray based measurements. In medical diagnostics, iodine is typically used as a contrast agent since it has a much higher attenuation coefficient than water or soft-tissues. Iodine-based solutions of Povidone-Iodine (Dynarex, #1416), Isovue-370 (Bracco Diagnostics, #NDC:0270-1316), Histodenz (Sigma Aldrich, #2158), and Diatrizoic Acid (Sigma Aldrich, #D9268) were tested as possible contrast-enhancing fluids. Povidone-iodine solutions are used as topical antiseptic, while Isovue-370, Histodenz, and Diatrizoic Acid are widely used to improve the visibility of internal bodily structures. The Isovue-370 stock solution was diluted with distilled water to create additional solutions of 1:2, 1:4, and 1:9 dilutions, since Isovue-370 is a very viscous solution.

The linear attenuation coefficient of the various iodine-based solutions and distilled water were measured from X-ray projections. The Hounsfield scale defined by CT number characterizes the small difference between different liquid attenuation levels. By definition, water has a CT number of zero and air has a CT number of -1000, since  $\mu_{air} = 0$ . Table 2 list the measured viscosity, density, and CT number for the tested contrast-enhancing fluids. Based on the measured properties and available quantity of solution, the experimental measurements were performed using the dilute solution of Isovue-370 prepared to a 20% volume fraction with distilled water. The dilute solution of Isovue-370 was fed to the pressure swirl atomizer using a rotary vane pump with pressure being maintained steadily by a pressure regulator. The operating pressure for the atomizers is approximately 20psi.

Liquid	Viscosity $10^{-6} [m^2/s]$	Density $[kg/m^3]$	CT number
Povidone Iodine	4.34	1022	500
Isovue-370	>5.0	1377	3200
33% Isovue-370	1.60	1121	2400
20% Isovue-370	1.26	1067	1700
10% Isovue-370	1.07	1010	900
Histodenz	0.99	1008	500
Diatrizoic Acid	1.10	1024	1200

Table 2: Comparative data on X-ray contrast-enhancing fluids

## X-ray CT Results

Measurements have been acquired both inside the atomizers and for a distance of approximately ten orifice diameters downstream. The results are time-averaged liquid concentration distribution,  $C$ . Figure 5 shows a cross sectional slice taken from the 3D reconstruction of liquid concentration distribution along the  $x=0$  plane for the 2 mm pressure swirl atomizer. The atomizers display spray characteristics typical of pressure swirl atomizers. A nominally axisymmetric hollow cone spray is formed immediately after the exit orifice with an air-cored vortex that extends to the top of the swirl chamber formed upstream of the exit orifice.

Spray profiles of liquid concentration along the  $x=0$  plane at different downstream distances of the exit orifice for the 2mm atomizers are shown in Figure 6. Note that there is some variation of the liquid concentration with azimuth angle.

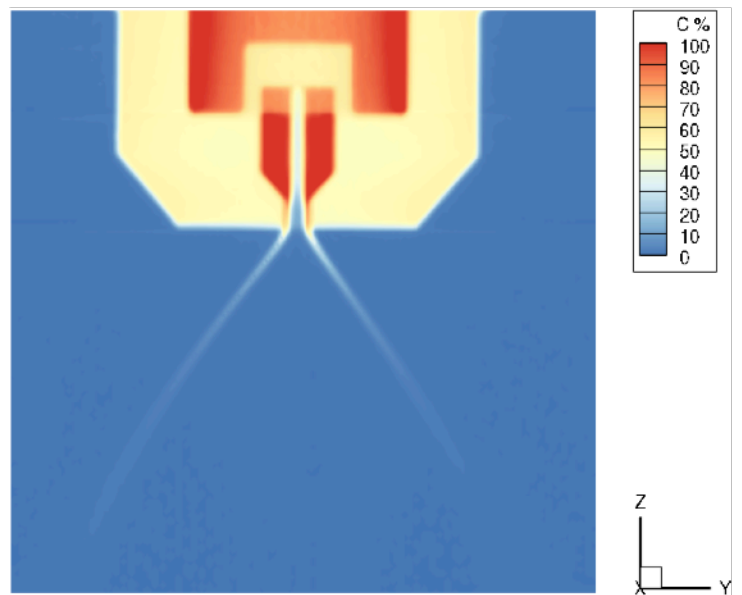


Figure 5: Cross-sectional slices of liquid concentrations distribution along  $x=0$  plane for the 2 mm atomizer

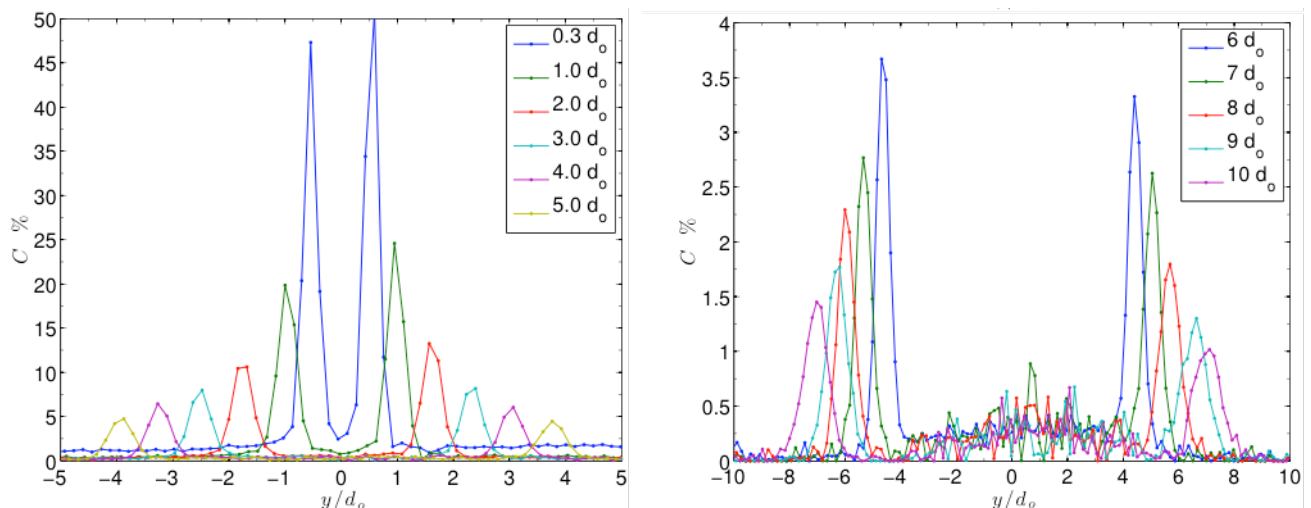


Figure 6: Spray profiles of liquid concentration distribution at different distances along the  $x=0$  plane for the 2mm atomizer

Figure 7 shows a series of cross-sectional contours of liquid concentration at different distances downstream from the exit orifice with a 3% liquid concentration cutoff level for ease of visualization. The contours demonstrate the nominally axisymmetric nature of the pressure swirl atomizer spray. Complex three-dimensional structures of the spray density distribution can be visualized using iso-surfaces of varying concentration as shown in Figure 7. Similar results have also been obtained for the 3 mm pressure swirl atomizer [2].

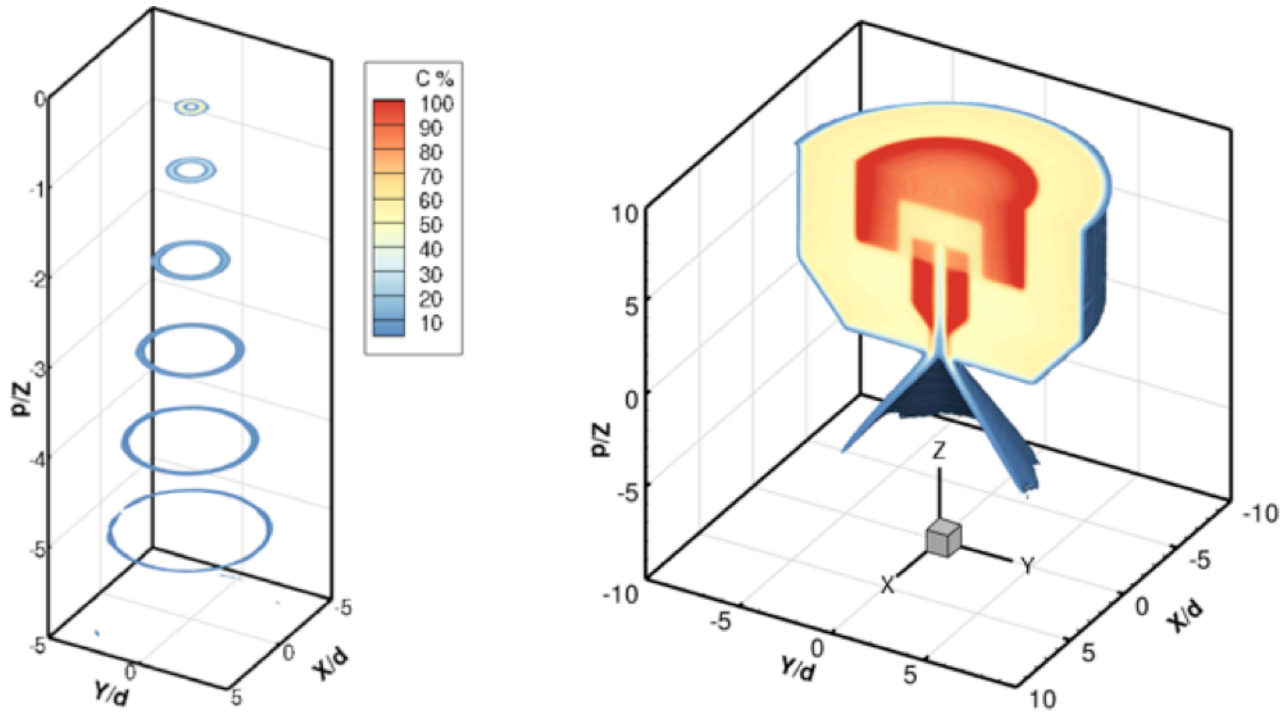


Figure 7: (a) Contours of liquid concentration at distances of  $Z/d = 0.3, 1, 2, 3, 4, 5,$  and  $6$  with a 3% concentration cutoff level for the 2 mm atomizer (b) Iso-surface of 3% liquid concentration and slice along  $x=0$  place with a 3% concentration cutoff level for the 2 mm atomizer

In addition, a scaled 1.5 mm and an occluded 2 mm pressure swirl atomizers were manufactured. The 1.5 mm atomizer provided a larger dynamic range of measurements, since it further reduced the amount of liquid accumulation along the chamber walls, while still providing adequate spatial resolution. The occluded 2 mm atomizer was manufactured to demonstrate the three-dimensional capabilities of the experimental technique. The asymmetric atomization of the occluded 2 mm atomizer was fully captured. X-ray CT allows us to investigate the 3D atomization properties and as manufacturing technologies advance, there is the possibility of manufacturing atomizers that are purposefully 3D.

### Model-based Evaluation of Artifact, and Correction Approach

Non-uniformity in liquid concentration profile across the nozzle of the atomizer, particularly in regions of high concentration of contrast agent, was thought to be due to beam hardening artifact (see some evidence of this in Figure 7, (b)). Although the error is small, the resulting inaccuracy can hinder comparison and validation across different measurement systems. Through experiment and simulation, we developed a detailed understanding of the effect, and propose a method to correct for the small inaccuracy.

The reduction in intensity (ADU) of x-rays passing through an object is given by

$$I = I_0 \exp(-\mu d)$$

This assumes monochromatic x-rays or no beam hardening. Here  $I$  is the measured ADU value with the object,  $I_0$  is the value without the object,  $\mu$  is the absorption coefficient, and  $d$  is the distance through the object. If there

is beam hardening, the initial layers of the material remove the soft, low-energy, x-rays. Thus thicker objects have less attenuation per unit thickness than thinner objects.

For projection images, beam hardening is usually not considered a problem. However it causes artifacts when a CT reconstruction is done because the reconstruction algorithm assumes the absorption as a function of distance obeys the above equation. If attenuation is measured as a function of thickness, and there is only one type of material in the object, for each intensity in the projection image it is known what the intensity would have been if there had been no beam hardening. Given the observed intensity of a pixel, we can change the intensity to the value it would have had without beam hardening, usually called the ‘water correction’.

Briefly, the steps are as follows:

- Measure the ADU values for a range of thicknesses of Isovue solution.
- Take the log of the ratio of the ADU value for each thickness divided by the ADU value with nothing in the path. This will be called the “log-ratio”.
- Plot the log-ratio as a function of thickness and fit the first few points to a second-order function. Assume the offset from zero for zero thickness is due to the attenuation caused by the walls of the step-wedge container. Take the linear value as the ‘correct’ value.
- In order to create a look-up table, list the ADU values ( $ADU_{measured}$ ) as a function of thickness. For each thickness, create linear ADU values ( $ADU_{corrected}$ ) using the relationship
- 

$$\ln\left(\frac{ADU_{corrected}}{I_0}\right) = -\mu d$$

$$ADU_{corrected} = I_0 \exp(-\mu d)$$

where  $\mu$  is the effective absorption coefficient for thin material.

- There are now two sets of values for each thickness; the values can be fit to an analytical function or a look-up table can be created for interpolation.

We have investigated the above approach using a step-wedge phantom. The phantom provides a range of different, known thicknesses of water and Isovue. When plotted as a function of thickness, the raw Analog-to-Digital units (ADU, or intensity) should follow an exponential curve. The results of our measured data are shown here using an acrylic sample holder and measuring over a roughly 100 pixel square region for each thickness.

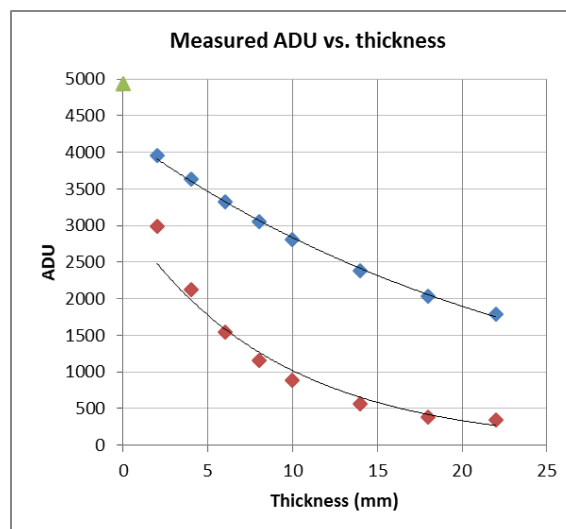


Figure 8 shows un-modified ADU values for the step-wedge phantom where blue is water and red is IsoVue. The green triangle is the background ADU value,  $I_0$ . The black lines are the exponential fits to the data. Water is fit fairly well and thus shows much less beam-hardening than IsoVue.

According to the above equations, the data should be exponential with thickness assuming no beam hardening. The fit lines do not go through the background point since the measured values include both the liquid and the step-wedge container. Also note that the values seem to have an asymptote greater than zero. We have also accounted for the presence of the step-wedge container, and calculate the ADU value that would have been obtained for each step of the step-wedge without the container.

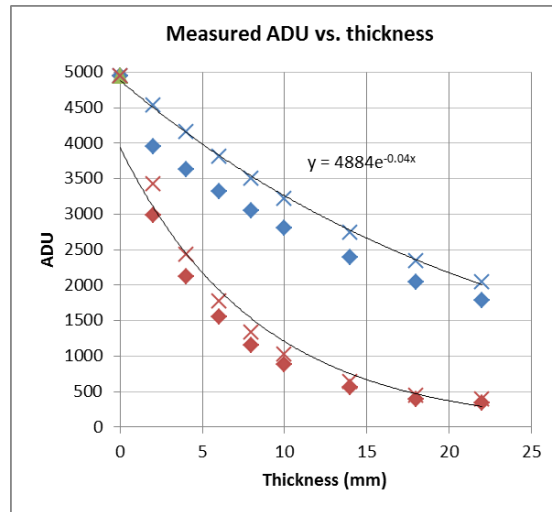


Figure 9 is the same as the previous plot modified such that the absorption of the step-wedge container has been removed. These new values are the crosses. The black trend-lines are exponential fits to the crosses. Note that the water data again fits fairly closely indicating little beam hardening.

From these experiments and additional model calculations, we could not find a fit that provided correction for ‘beam hardening’ for the Isovue thickness range that we measured. We have therefore determined that beam hardening is not the primary cause of inaccuracy in the reconstructed attenuation coefficients of the spray. Other possible causes of error include detector calibration offset, x-ray scatter and off-focal radiation (x-rays emanating from the x-ray tube, but not confined to the focal spot, which creates a background ‘haze’ or offset across the projection images). Through simulation, we have found that a correction offset of 285, or ~6% of the maximum value recorded in air (unattenuated signal) leads to linear response of both Isovue and water as a function of thickness, as shown below.

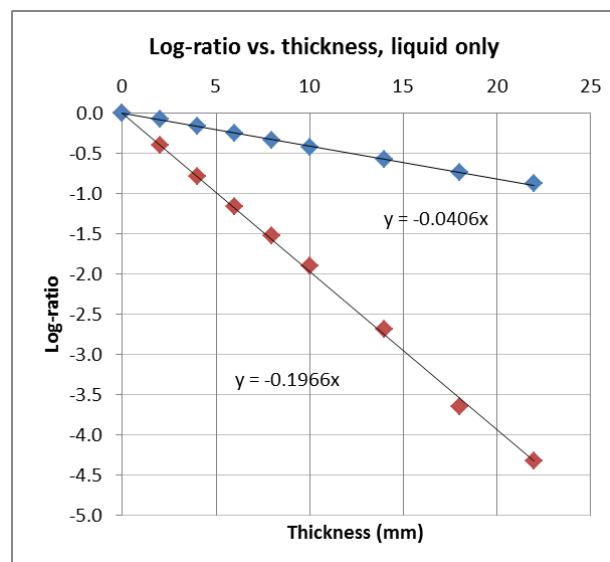


Figure 10 Linear fit resulting from uniform offset correction of the data amounting to  $\sim 6\%$  of the maximum recorded value in each projection image. Note that a frame-to-frame calibration is also required to correct for temporal variations in the x-ray tube output.

Examples of image pairs without and with the linearity correction are shown below. The reconstructed slices are through two vials containing IsoVue, and show the impact on image quality if correction is neglected.

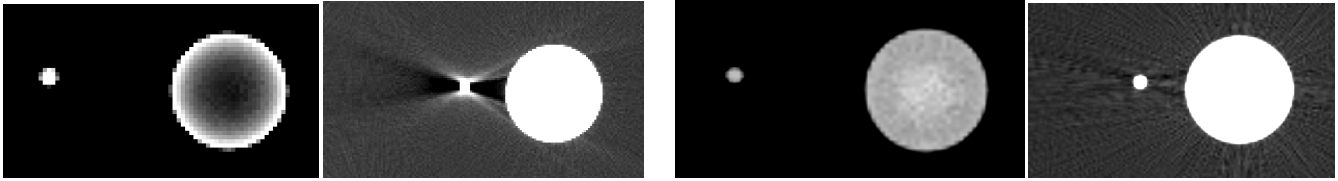


Figure 11 Images of the Isovue-filled nozzle and a small vial also filled with Isovue. Both objects should have the same attenuation value. (left) Two different display values (window/level) applied to the same image show difference in mean signal between nozzle and vial, the cupping artifact (non-uniformity within the nozzle), and decrease in background signal between the nozzle and the vial. (right) The same data reconstructed with our linearity correction. All of the artifacts have been significantly reduced.

With no linearity correction, the difference between the center of the nozzle and the vial is  $\sim 22\%$ . After correction, the difference between the center of the nozzle and the vial is  $\sim 0.2\%$ . This work validates the accuracy of the reconstructed density measurements based on the measured attenuation values, and highlights the need for careful measurement and complete understanding of the x-ray acquisition hardware system.

## Experimental Validation

To validate the experimental measurements from the X-ray CT based system conventional shadowgraphy and PLIF optical measurements were conducted at the U.S Army Research Laboratory's Spray and Combustion Research Laboratory. The experimental rig constructed at ARL permits 2D optical imaging, which can be compared directly with 2D projection images from Stanford 3D imaging system. Shadowgraphy is an optical techniques which only provides a qualitative comparison of the spray; however, it can resolve droplets and provide basic droplet analysis. PLIF offers a direct quantitative comparison of the measured liquid concentration for the X-ray CT measurements. Preliminary shadowgraphy and PLIF measurements have been acquired for the same 2 mm pressure swirl atomizer used in the Stanford X-ray based measurements. Future measurements require proper calibration of the Shadowgraphy and PLIF measurements to provide an accurate comparison.

For the shadowgraphy measurements, a Photron SA5 Fastcam camera recorded the spray at 40,000 frames per second using an exposure time of  $1 \times 10^{-6}$  seconds. A LED light source was located directly across the chamber from the camera and was positioned behind a diffuser to provide a consistent intensity of light across the camera. In order to effectively compare images from shadowgraphy, software was used to create a time-averaged image from 2500 frames of the spray from 5 different data sets, which corresponds to an averaging over 0.0625 seconds. Time averaging gave an accurate image of the average spray cone angle and perimeter of the conical spray. Figure 12 shows a direct comparison of the time-averaged shadowgraphy measurements with a 2D projection of the X-ray CT measurement. The two measurements result in slightly different spray cone angles, but qualitatively display similar spray characteristics. Detailed comparison is described in reference [3].

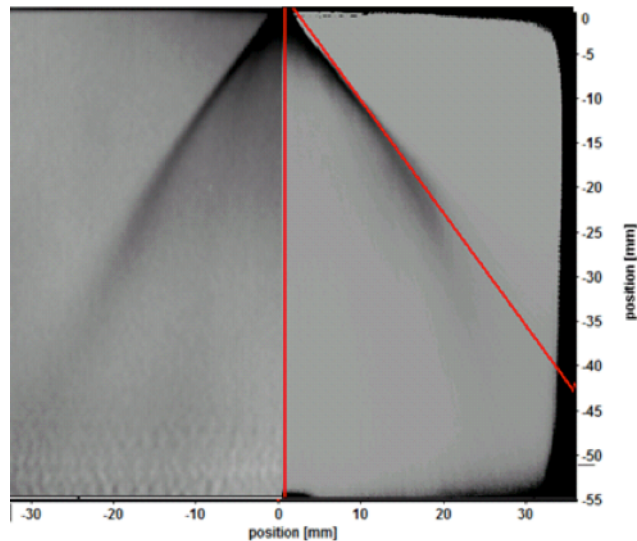


Figure 12: X-ray CT 2D projection (left) vs. time-average Shadowgraphy 2D image (right)

Shadowgraphy is limited in its ability to examine the near-nozzle region. The spray is sufficiently dense to reduce pixel intensity to zero, so the average spray density cannot be determined in the near-nozzle region. However, Planar Laser-Induced Fluorescence (PLIF) measurements provide a direct comparison. Figure 13 shows a comparison of the measured profile concentration for the PLIF measurements vs. the X-ray CT measurements. The preliminary comparison shows a difference in spray cone angle, but recently new processed X-ray CT measurements display similar spray cone angle. A better agreement is expected to be achieved with new properly calibration measurements.

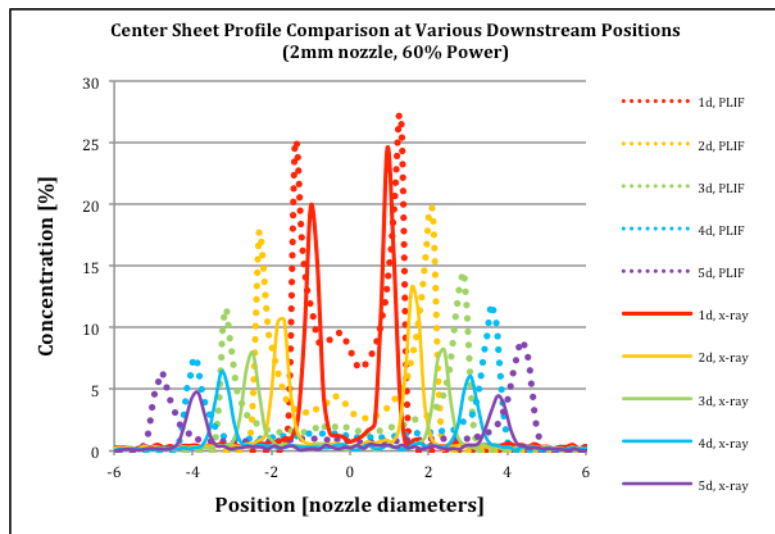


Figure 13: Concentration profile comparison

## Conclusion and Summary

At the end of Year 1 of this project, we have completed our specific aims and have developed an optimized CT system design for near-field spray imaging. Further improvements to the system for spray imaging need to include a higher-resolution detector with a very low noise floor, 0.1 mm or smaller focal spot, and a hardware shutter for very short exposure times. Because the technique is inherently non-optical, understanding the fluid flow within the nozzle provides unique access to this critical region where flow features from non-uniformities induced by cavitation or separation can have major impact on downstream atomization. Quantification of the experimental uncertainty of the technique will be determined by detailed analysis of the results, reproducibility studies, and comparison to optical measurements conducted in the ARL Combustion Research Laboratory.

## References

- [1] Lefebvre, A. H., 1989, *Atomization and Sprays*. Hemisphere Publishing Co., New York.
- [2] Vasquez Guzman, P. A., Eaton, J., Fahrig, R., Coletti, F., and Benson, M., 2014, “Near-Field Spray Measurements Using X-ray Computed Tomography,” *ILASS Americas, 26<sup>th</sup> Annual Conference on Liquid Atomization and Spray Systems*.
- [3] Lee, Z., et al. 2014. “A Comparison of Shadowgraphy and X-ray Computed Tomography in Liquid Spray Analysis.” *ASME 2014 International Mechanical Engineering Congress and Exposition*.